XVI International Conference on Durability of Building Materials and Components
DBMC 2023, China
K.F. Li and D.P. Fang (Eds)

Hysteretic and Scanning Behaviors of Water Vapor Sorption in Hardened Cement Pastes

Zhen Wang[1] **and Kefei Li**[1]

[1]Department of Civil Engineering, Tsinghua University, Beijing 100084, PR China, wangzhen19@tsinghua.edu.cn (Zhen Wang, Corresponding author), likefei@tsinghua.edu.cn (Kefei Li)

Abstract. *Water in the multiscale porous microstructure of cement-based materials is closely related to multiple deterioration processes, hence significantly influences the durability of concrete structures in atmospheric environment. Water vapor sorption is the key tool for characterizing the hygroscopic properties of cement-based materials, also a promising technique for exploring their nanopore structures. The significant hysteresis between different sorption branches is stemmed from the complexity of interconnecting pore system and concurrence of different physical phenomena. In this study, the hysteretic and scanning behaviors of water vapor sorption in hardened cement pastes are measured with a dynamic vapor sorption instrument, and investigated to provide new insights into the path-dependency of sorption behaviors on humidity history and resolve the overall sorption hysteresis into contributions from different phenomena.*

Keywords: *Water vapor sorption; Hardened cement pastes; Humidity; Hysteresis; Scanning curves*

1 Introduction

Cement-based materials contain considerable amount of water in their multiscale porous microstructure, which is in dynamic equilibrium with the fluctuating humidity of atmospheric environment. As an integral part of the material itself, water is closely related to multiple deterioration processes occurring in cement-based materials, significantly influencing the durability of concrete structures (Baroghel-Bouny, 2007). Water vapor sorption isotherm is the fundamental characterization of the moisture properties of cement-based materials, depicting the multivalued relationship between equilibrium moisture content and relative humidity. Significant hysteresis between different sorption branches originates from the complexity of nanoscale pore structure and the deformation of hydrophilic substrate during drying and wetting processes, manifesting the path-dependency of moisture properties on humidity history of cement-based materials. Study on the scanning curves cutting across the hysteresis region is indispensable for describing the influence of humidity history on sorption behaviors and understanding the underlying mechanisms. In this study, we conducted a series of measurements on the water vapor sorption isotherms and scanning curves of hardened cement paste with dynamic vapor sorption instrument. It was found that the first desorption isotherm initiated from saturated state is of particular significance compared with the following ones. We have analyzed the hysteretic and scanning behaviors and discussed the path-dependency of sorption behaviors. The overall sorption hysteresis has been resolved into contributions from different physical phenomena for further modeling.

2 Materials and Experiments

The hardened cement paste was prepared with reference ordinary Portland cement P.I. 42.5 with water-to-cement ratio of 0.4. Deionized water was used to mix the cement, and the formed paste was cast into plastic tubes with screw caps. Parafilm was used to seal the tubes in order to minimize water loss. The tubes were gently rotated before initial setting, and then stored in a curing chamber at 20 °C and 95%RH. Samples were sliced with diamond saw into discs of 2 mm in thickness at the age of ~150 days, and then immersed in saturated limewater. The continued hydration for a few months was found to have limited impact on measured sorption curves.

Sorption isotherms were measured gravimetrically with a dynamic vapor sorption analyzer DVS-Adventure produced by Surface Measurement Systems, UK, which monitors the mass change over time of a sample kept in a nitrogen flow with accurately controlled relatively humidity and temperature. The microbalance is located on the top of the device, while sample pan and reference pan are suspended from the ends of balance beam into chambers flowed with nitrogen carrying specified amount of water vapor. The whole device is placed in an incubator with precisely controlled temperature. The microbalance with a sensitivity of 1 μg was calibrated with a certificated weight, and its baseline stability was checked before the experiments were carried out. The proportion of dry and saturated nitrogen flow with a total rate of 200 sccm is regulated with control precision of 0.1 sccm by two mass flow controllers calibrated with saturated LiCl, NaBr, and KCl solutions with reference deliquescence points from (Greenspan, 1977). The sorption temperature is controlled at 25 °C with a Eurotherm controller and a Pt100 probe (± 0.1 °C).

Before each experiment, the disc of paste was taken out from limewater and quickly crushed into grains sieved between 200 μm and 500 μm. Two initial states are specified: non-saturated and saturated. For non-saturated samples, the obtained grains were directly loaded into the sorption analyzer and equilibrated at 98%RH; for saturated samples, a few drops of limewater were added to the grains and kept for about 1 h in sealed condition before the grains were loaded into the device and underwent 98%RH equilibration to remove free water. The mass of grains used for each sorption experiment was more than 30 mg after the first 98%RH stage. For each RH step, the ending criterion was set to be $|\mathrm{d}m/\mathrm{d}t| \leq 0.001$ wt.%·min^{-1} kept for 10 minutes. The sorption kinetics curves at each sorption step were fitted with Eq. (1) to acquire the extrapolated sample mass at "infinite" time:

$$m(t) = m(0) + \sum_{i=1}^{3} q_i \left[1 - \exp\left(-K_i t^{\alpha_i}\right)\right] \tag{1}$$

where $m(t)$ is the mass of sample (mg), t is the time (min), q_i (mg), K_i, α_i are fitting parameters. The extrapolated mass at 0%RH was chosen as the reference mass for calculating moisture content. Different RH sequences were implemented to measure the hysteretic and scanning behaviors of sorption in cement pastes, including multiple desorption-adsorption cycles, ascending scanning sequence, and descending scanning sequence, which will be introduced in the following section.

3 Results

The desorption isotherms record the moisture content as the ambient RH decreases, while the adsorption isotherms are measured with increasing RH. At the same RH, higher moisture content is always measured in desorption than in adsorption, which is referred to as the hysteresis of sorption. To start with, the first desorption-adsorption isotherms (98%-0%-98%RH) of initially saturated sample and non-saturated sample are shown in Fig. 1. The first desorption isotherm of initially saturated sample is notably higher than that of non-saturated sample above 40%RH, while the difference is eliminated below 30%RH. The first adsorption isotherms of two cases have minor difference between each other below 70%RH, while the gap is relatively larger above 70%RH. The sharp drop during desorption in 40-30%RH has been attributed to the spontaneous cavitation of liquid water under high tension (Maruyama et al., 2018; Rastogi et al., 2022), hence, we may speculate that no liquid water may exist below 30%RH, and the difference between initially saturated and non-saturated samples arises from different amount of liquid water in pore system between two cases, which is identifiable by the difference of moisture contents at 98%RH. The overlap of desorption isotherms in low-RH range and adsorption isotherms below 70%RH suggests that initially saturated or not does not affect the sorption of water molecules on substrate.

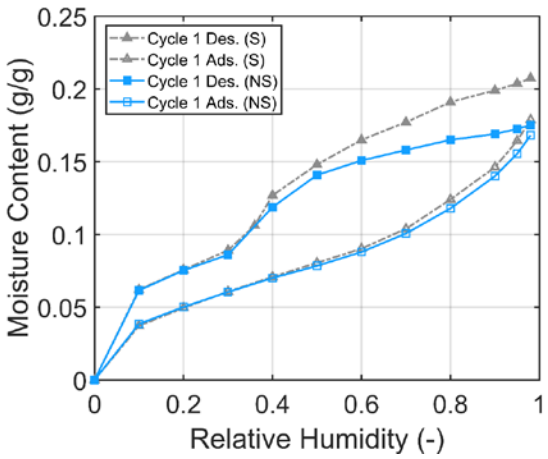

Figure 1. The isotherms of the first desorption-adsorption cycle of initially saturated sample (S) and non-saturated sample (NS).

Two additional desorption-adsorption cycles were measured for non-saturated samples. The slopes of sorption cycles are given in Fig. 2 to facilitate analysis. It can be observed that there is little difference between isotherms of the second and the third cycle which had previously underwent 0%RH equilibration, while the desorption isotherms of the first cycle are distinct from the following ones. During the first desorption of initially saturated samples, more water was desorbed in the range of 50-30%RH and 10-0%RH, which is respective related to cavitation phenomenon and desorption from substrate surface or hydration products (Baquerizo et al., 2016; Jennings et al., 2015), while similar isotherm slopes with following cycles is observable in other RH ranges. All adsorption isotherms are close to each other below 70%RH, but less water is adsorbed with increasing number of cycles in the range of 70-90%RH. In the range of

90-98%RH, the adsorption isotherm slopes of the first two cycles are similar, while that of the third cycle is lower. These phenomena indicate that the first desorption isotherm has a particular significance compared to those in subsequent cycles which have previously been equilibrated at 0%RH.

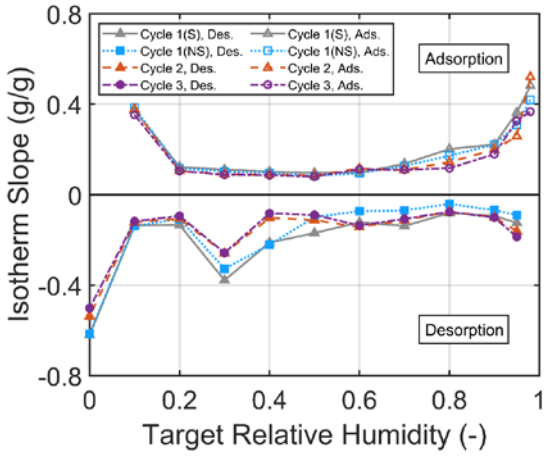

Figure 2. The slopes of multiple-cycle isotherms.

The ascending scanning curves of non-saturated sample are given in Fig. 3. Curves with higher starting RH are measured earlier. Attention should be paid to curves with starting points below 40%RH since these points are not affected by whether or not the initial saturation is conducted. Two key points can be found from these data: the first is that ascending scanning curves with starting points in 10-30%RH overlap with each other; the second is that the ascending scanning curves starting from 0%RH, i.e. the adsorption isotherm, detaches from the above-mentioned cluster of overlapping curves, and the gap between them persists until it starts to decrease more notable with rising RH above 60%RH, and becomes very small at 98%RH.

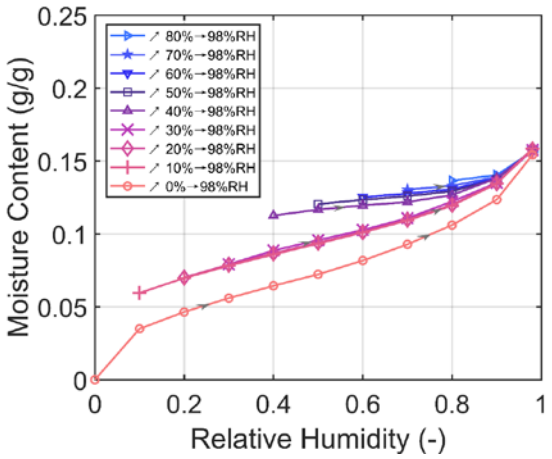

Figure 3. The ascending scanning curves of non-saturated sample.

We have also measured the ascending scanning curves with starting points above 40%RH

of initially saturated sample, which are shown in Fig. 4. Similar with those in Fig. 3, the ascending scanning curves with starting points above 40%RH increase almost linearly and tend to converge above 80%RH. It should be noted that for each ascending scanning curve with starting point above 70%RH, the moisture content at 98%RH lowers with the RH of starting point, which indicates that the part of water induced by initial saturation is gradually discharged.

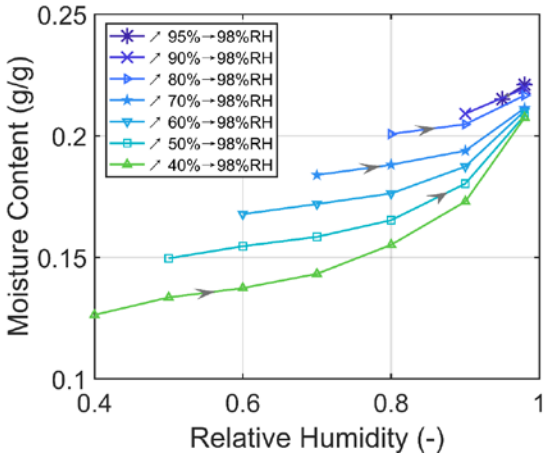

Figure 4. The ascending scanning curves with starting points above 40%RH of initially saturated sample.

The descending scanning curves measured after the multiple sorption cycle are illustrated in Fig. 5, with lowest starting RH measured first. It is noticeable that the curve with starting point at 50%RH overlaps with that starts at 35%RH, while cavitation-related drop and lifted moisture content at low RH range below 30%RH are observable for curves with higher starting points.

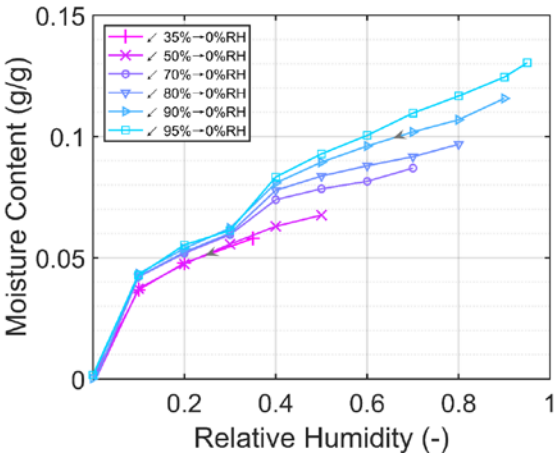

Figure 5. The descending scanning curves measured after the multiple sorption cycles.

4 Discussions

4.1 Path-dependency of Sorption Behaviors

Physisorption on pore walls, capillary condensation, and the possible substrate swelling are the

main mechanisms at work during adsorption, while the desorption isotherms are complicated by the metastable water in geometrically confined "ink-bottle" pores, also the substrate shrinkage occurring when the RH is quite low. The results described in the previous section indicate that the sorption behavior is dependent on the path it has previously undergone. The first desorption isotherm of initially saturated sample is particularly significant because of two key points: more water is desorbed during cavitation between 50-30%RH and from the surface and inner structures of hydration products below 10%RH. Moreover, the ascending scanning curves with different starting points exhibit different scanning behaviors, indicating that different physical phenomena are at play. When the RH remains above 40%RH, the main contributing factors are the release and filling of liquid water, which can be described by the “ink-bottle” effect (Ishida et al., 2007) arising from the geometrical confinement posed on water in pore cavities by water in narrow pore necks as RH decreases, and multilayer adsorption and capillary condensation in previously emptied pores as RH increases. When the RH is below 30%RH, no liquid water may persist in pore structures due to the cavitation phenomenon as the negative pressure exerted on the stretched water in pore cavities exceeds the limit of stability, the overlapping of ascending curves with starting points in 10-30%RH suggests that the pure physisorption is probably reversible. The gap between adsorption isotherm with starting RH at 0%RH and ascending curves with starting point at 10%RH is indicative of the water loss from inner structures of hydration products at 0%RH which cannot be recovered unless the RH is high enough. The descending curves of samples previously underwent drying at 0%RH have also suggested this point. These path-dependencies need to be further studied and considered in the modeling of mass transport in cement-based materials.

4.2 Resolving Sorption Hysteresis

The sorption hysteresis between desorption and adsorption isotherms manifests the complexity of the microstructure of cement-based materials. As aforementioned, different physical phenomena are involved in different RH ranges, it is hence necessary to resolve the total sorption hysteresis exhibited in Fig. 1 into contributions from different phenomena in order to establish an accurate model for describing and predicting sorption behaviors of cement-based materials. To begin with, the contribution from substrate shrinkage in 10%-0%RH, which is responsible for the low-RH hysteresis below 30%RH in Fig. 1 (Thommes et al., 2015), can be isolated by measuring the ascending scanning curve with starting point at 10%RH before the adsorption isotherm started at 0%RH, and deducted from desorption isotherms by subtracting the width of gap between two curves. Meanwhile, during desorption, confined liquid water are discharged through two mechanisms: cavitation and pore-blocking (Nguyen et al., 2011). Cavitation occurs in a narrow RH range, so the cavitation-related drop can be directly subtracted from moisture content from the desorption isotherms. However, in adsorption branch, the gradual development of cavitation-related water, which is demonstrated in Fig. 5, should also be deducted. After deducting the effect of substrate shrinkage and cavitation, the remaining difference between desorption and adsorption isotherms is contributed by the pore-blocking effect in ink-bottle pores. This resolving of sorption hysteresis should be further improved to be applied in numerical modeling.

5 Conclusions

In this study, we measured the water vapor sorption isotherms of hardened cement paste in multiple desorption-adsorption cycles, together with ascending scanning curves and descending scanning curves cutting across the hysteresis region. We found that the first desorption isotherm initiated from saturated state is of particular significance with more water desorbed in 50-30%RH and 10-0%RH, while limited difference was observed for isotherms in following cycles. The scanning behaviors are path-dependent, and indicative of which mechanisms are at play. The total sorption hysteresis can be resolved into contributions from substrate shrinkage, cavitation, and pore blocking phenomenon with information from scanning curves. These results show that the knowledge on hysteretic and scanning behaviors and the interpretations of underlying mechanisms are indispensable for the accurate modeling of hygroscopic behaviors, nanopore structures, and transport properties of cement-based materials. The dependency of scanning behaviors on previous humidity history should be fully addressed due to their crucial importance for concrete structures exposed to humidity fluctuations in atmospheric environments. Further studies on the path-dependency of scanning behaviors are required for improved comprehension and modeling of water vapor sorption behaviors in cement-based materials.

Acknowledgements

This research is supported by the National Natural Science Foundation of China (Grant No. 52038004).

ORCID

Zhen Wang: https://orcid.org/0000-0001-8124-6712
Kefei Li: https://orcid.org/0000-0003-1635-6362

References

Baquerizo, L. G., Matschei, T., & Scrivener, K. L. (2016). Impact of water activity on the stability of ettringite. *Cement and Concrete Research, 79*, 31-44.

Baroghel-Bouny, V. (2007). Water vapour sorption experiments on hardened cementitious materials. Part I: Essential tool for analysis of hygral behaviour and its relation to pore structure. *Cement and Concrete Research, 37*(3), 414-437.

Greenspan, L. (1977). Humidity fixed points of binary saturated aqueous solutions. *Journal of Research of the National Bureau of Standards Section A: Physics and Chemistry, 81A*(1), 89-96.

Ishida, T., Maekawa, K., & Kishi, T. (2007). Enhanced modeling of moisture equilibrium and transport in cementitious materials under arbitrary temperature and relative humidity history. *Cement and Concrete Research, 37*(4), 565-578.

Jennings, H. M., Kumar, A., & Sant, G. (2015, Oct). Quantitative discrimination of the nano-pore-structure of cement paste during drying: New insights from water sorption isotherms. *Cement and Concrete Research, 76*, 27-36.

Maruyama, I., Rymeš, J., Vandamme, M., & Coasne, B. (2018). Cavitation of water in hardened cement paste under short-term desorption measurements. *Materials and Structures, 51*(6), 159.

Nguyen, P. T. M., Do, D. D., & Nicholson, D. (2011). On The Cavitation and Pore Blocking in Cylindrical Pores with Simple Connectivity. *The Journal of Physical Chemistry B, 115*(42), 12160-12172.

Rastogi, M., Müller, A., Haha, M. B., & Scrivener, K. L. (2022). The role of cavitation in drying cementitious materials. *Cement and Concrete Research, 154*, 106710.

Thommes, M., Kaneko, K., Neimark, A. V., Olivier, J. P., Rodriguez-Reinoso, F., Rouquerol, J., & Sing, K. S. W. (2015). Physisorption of gases, with special reference to the evaluation of surface area and pore size distribution (IUPAC Technical Report). *Pure and Applied Chemistry, 87*(9-10), 1051-1069.